9.3: LARGE SIGNAL PROPERTIES OF NON-DEGENERATE VARACTOR PARAMETRIC AMPLIFIERS

DARRELL JACKSON

The Boeing Company, Seattle, Washington

Parametric amplifiers, in common with many other non-linear devices, exhibit peculiar and perhaps useful properties when operated at high signal levels. For example, abrupt switching between various modes of operation is sometimes observed, and simultaneous oscillation at two different frequencies may occur under certain conditions. A satisfactory quantitative description of many of these phenomena is obtainable through the use of the simplified circuit model shown in Figure 1. The signal

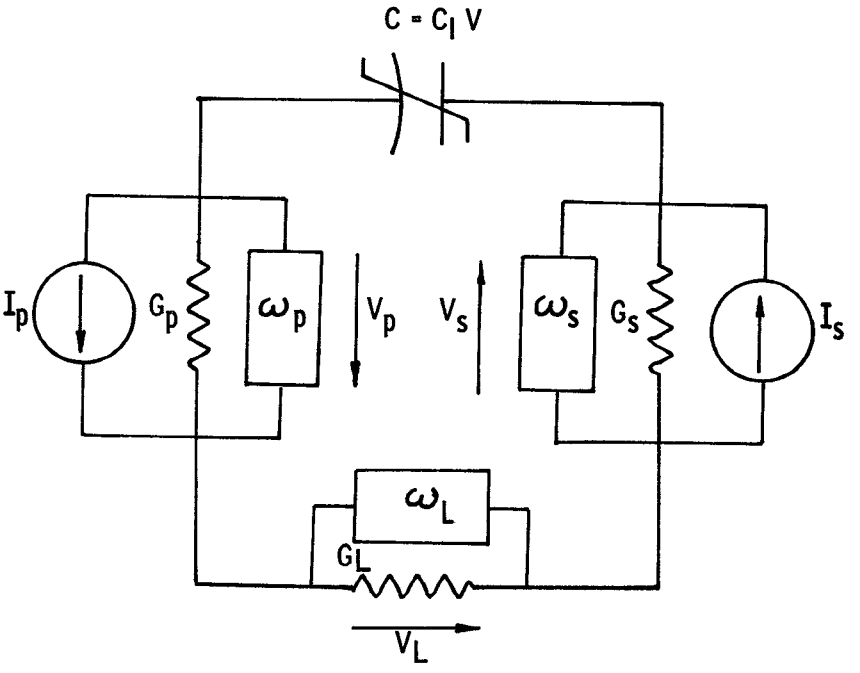

Fig. 1. Idealized parametric circuit.

source is represented by a current generator, I_s, of frequency ω_s, together with conductance G_s. The pump source consists of I_p and G_p at the pump frequency ω_p. Mixing takes place in a lossless non-linear capacitor with the simple characteristic $C = C_1 V$. Output power is dissipated at frequency ω_s in conductance G_s. Depending on the type of operation desired, ω_L may be either the sum or difference of ω_s and ω_p. The rectangular boxes labeled ω_s, ω_L, and ω_p represent ideal bandpass filters which are included to insure that voltages at only the three frequencies of interest appear across the varactor.

If ω_L is taken as the sum of ω_s and ω_p, the circuit will function as a non-inverting up-converter. The admittances seen by the signal and pump sources are:

$$Y_s = \frac{\omega_s \omega_L C_1^2 V_p^* V_p}{2G_L}, \tag{1}$$

and

$$Y_p = \frac{\omega_p \omega_L C_1^2 V_s^* V_s}{2G_L}, \tag{2}$$

where V_s and V_p are rms phasor quantities representing the components of varactor voltage at ω_s and ω_p. These expressions are of the form used by Kotzebue in analyzing the large signal properties of the negative resistance parametric amplifier, and are valid for all values of V_s and V_p for the circuit model chosen. Since these admittances are real, the Manley-Rowe formula can be used to obtain the following gain and voltage relations:

$$\frac{P_L}{P_s} = \frac{\omega_L}{\omega_s} \frac{4}{Y_s/G_s + 2 + G_s/Y_s}, \tag{3}$$

$$V_p V_p^* = \frac{2}{G_p}\left[P_p - \frac{1}{2}\frac{\omega_p}{\omega_L} P_L \pm \sqrt{P_p\left(P_p - \frac{\omega_p}{\omega_L} P_L\right)}\right]. \tag{4}$$

P_p and P_s are available signal and pump powers, and P_L is the actual load power dissipated in G_L. Relations (1), (2), and (3) make it possible to calculate output power versus available signal power for various pump powers. Rather than use these equations in their present form, it is convenient to write them in terms of the dimensionless, normalized powers defined below:

$$P_s = \frac{\omega_p \omega_L C_1^2 P_s}{G_s G_p G_L}, \tag{5}$$

$$P_p = \frac{\omega_s \omega_L C_1^2 P_p}{G_s G_p G_L}, \tag{6}$$

$$P_L = \frac{\omega_s \omega_p C_1^2 P_L}{G_s G_p G_L}. \tag{7}$$

Using (1), (3), (5), (6), and (7)

$$\frac{P_L}{P_s} = \frac{4}{Y_s/G_s + 2 + G_s/Y_s} \quad , \tag{8}$$

$$Y_s/G_s = P_p - \frac{1}{2} \; P_L \pm \sqrt{P_p \; (P_p - P_L)}. \tag{9}$$

Figure 2 shows curves of P_L vs. P_s calculated using (8) and (9). Of particular interest is the presence of loops for $P_p > 2$. These loops give

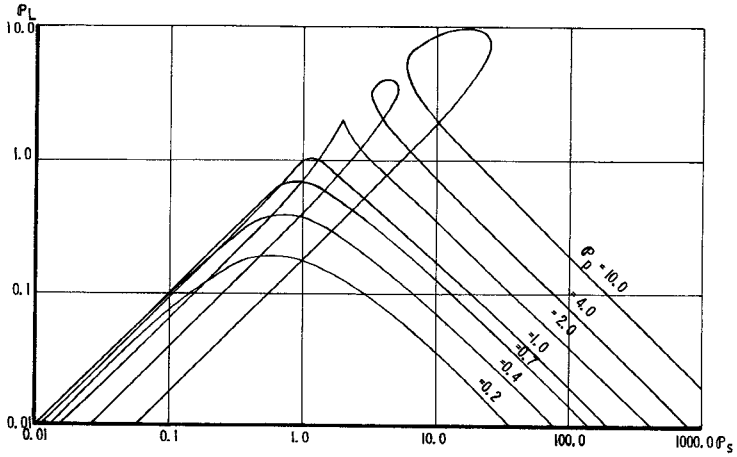

Fig. 2. Normalized power curves for non-inverting up-converter.

rise to switching and hysteresis effects which could prove useful in logic circuitry. The shape of these curves has been verified experimentally using a parametric circuit operating in the high-frequency range; and, as Figure 3 shows, agreement between theoretical and experimental curves is good.

For the inverting converter ($\omega_L = \omega_p - \omega_s$), the relevant normalized relations are:

$$\frac{P_L}{P_s} = \frac{4}{|Y_s|/G_s - 2 + G_s/|Y_s|} \quad , \tag{10}$$

$$Y_s/G_s = -\left[P_p - \frac{1}{2} \; P_L \pm \sqrt{P_p \; (P_p - P_L)}\right]. \tag{11}$$

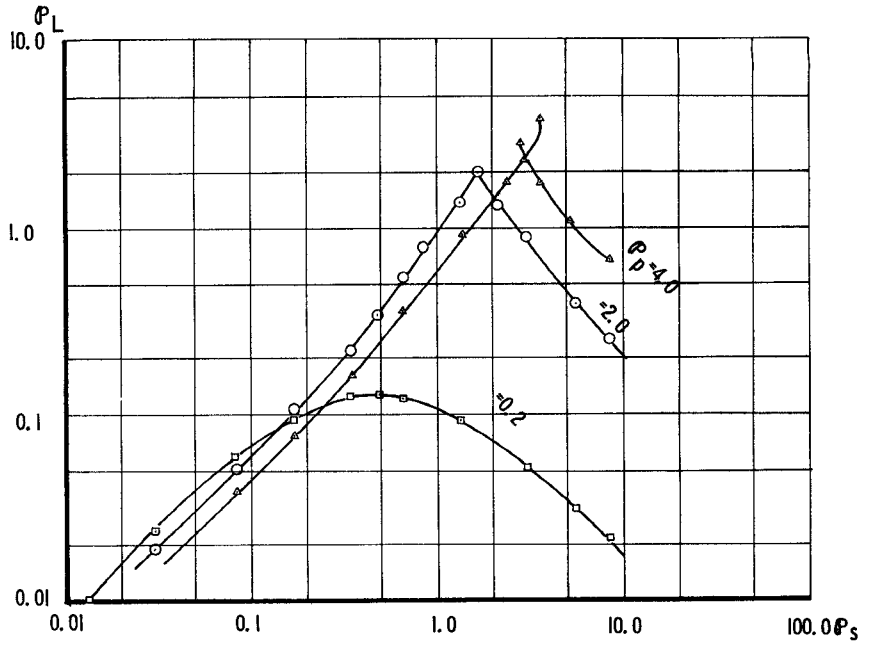

Fig 3. Experimental curves for non-inverting up-converter.

Since the signal source sees a negative admittance, stable operation is possible only when $|Y_s| < G_s$. Curves of P_L vs P_s for which $|Y_s| < G_s$ are shown as solid lines in Figures 4 and 5. Unstable curves, for which $|Y_s| > G_s$, are shown as broken lines in Figure 5. For $P_p > \frac{1}{2}$, the stable curves show a finite power output when $P_s = 0$. This oscillator output power can be found from (11), and is given by

$$P_L = -2 + 2\sqrt{2P_p} \quad , \quad P_p > \tfrac{1}{2} . \tag{12}$$

This function is plotted in Figure 6 together with measured values of oscillator output. Agreement is again very good. Except for a difference in definition of terms, (12) is the same as one found by Kotzebue for the oscillating negative resistance amplifier. That this should be so is easily seen by comparing the two circuit configurations.

Normalized power curves can be calculated for the non-inverting down-converter ($\omega_L = \omega_s - \omega_p$) by using the following relations.

$$\frac{P_L}{P_s} = \frac{4}{Y_s/G_s + 2 + G_s/Y_s} \quad , \tag{13}$$

$$Y_s/G_s = P_p + \frac{1}{2} P_L \pm \sqrt{P_p (P_p + P_L)} . \tag{14}$$

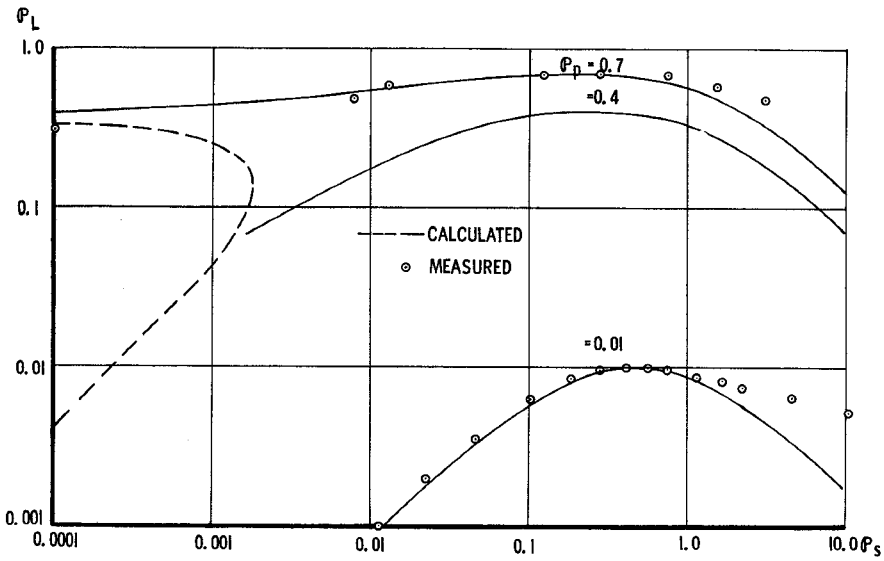

Fig. 4. Normalized power curves for inverting converter.

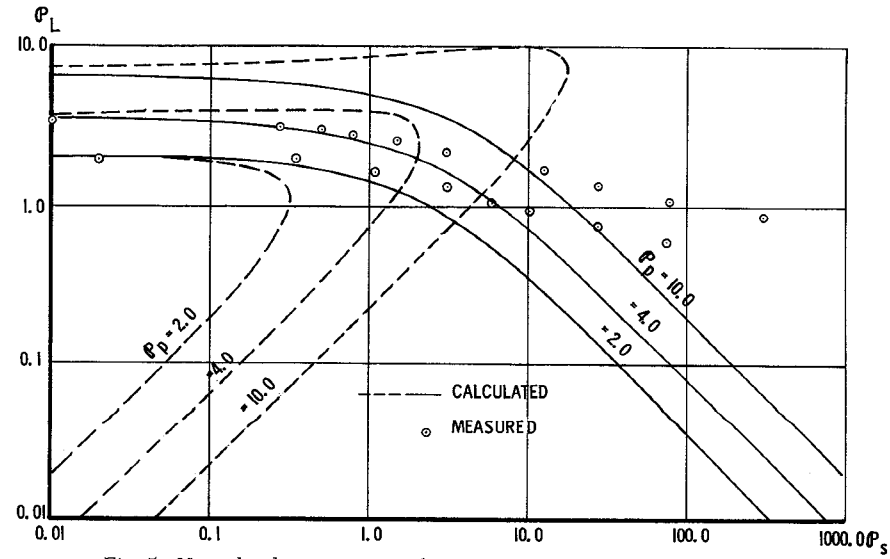

Fig. 5. Normalized power curves for inverting converter.

The pump generator sees a negative input admittance for this circuit; as a consequence, stable operation is possible only on those curves shown as solid lines in Figure 7 (on these curves, $|Y_p| < G_p$).

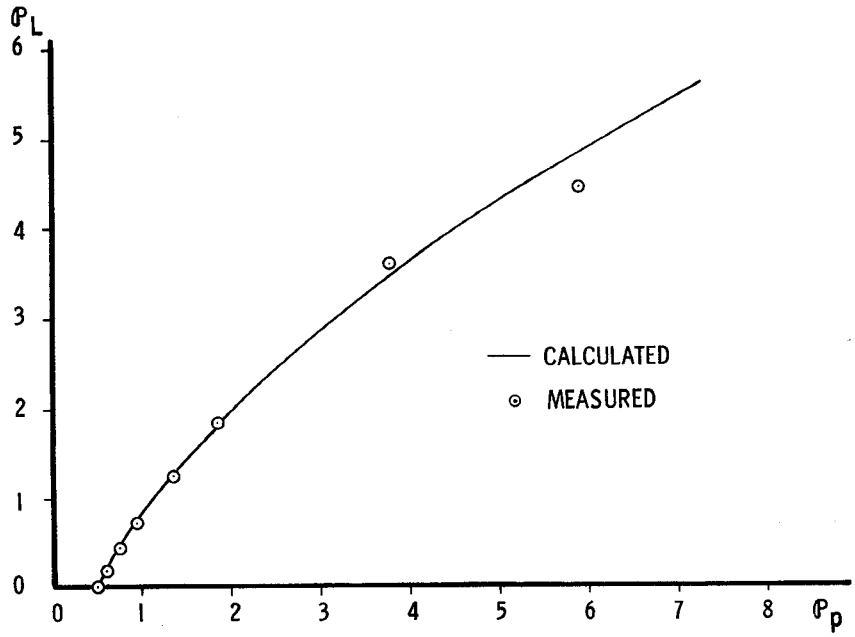

Fig. 6. Oscillator output power vs. pump power.

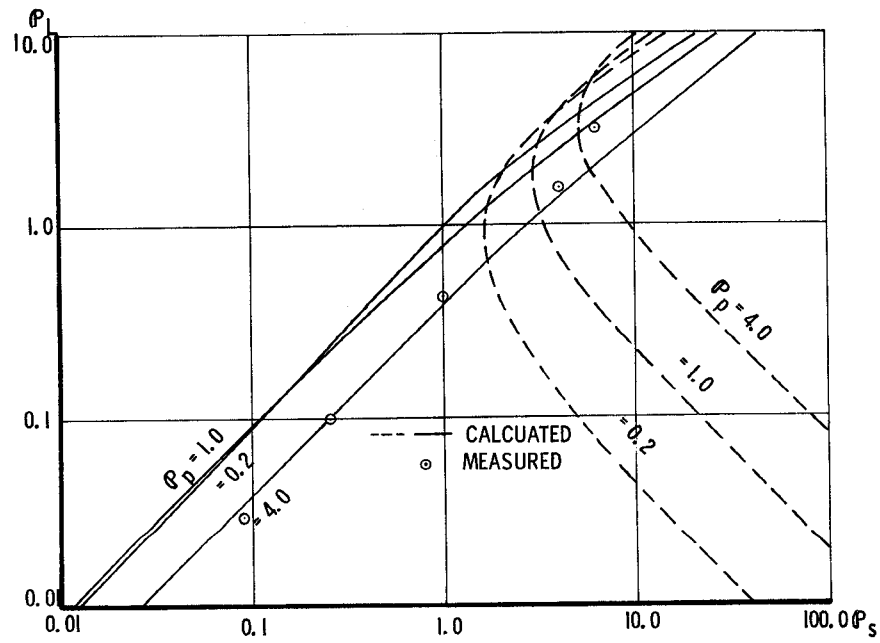

Fig. 7. Normalized power curves for non-inverting down-converter.